

In Situ X-ray Absorption of a Carbon Monoxide–Iron Porphyrin Adduct Adsorbed on High-Area Carbon in an Aqueous Electrolyte

In Tae Bae and Daniel A. Scherson*

Ernest B. Yeager Center for Electrochemical Sciences and the Department of Chemistry, Case Western Reserve University, Cleveland, Ohio 44106-7078

Received: September 26, 1997; In Final Form: January 12, 1998

The electronic and electrochemical properties of a carbon monoxide–FeTMPP adduct (FeTMPP = (5,10,15,20-tetrakis[4-methoxyphenyl]-21*H*,23*H*-porphine)iron(II)) adsorbed on Black Pearls (BP) high-area carbon have been examined in situ in 0.05 M H₂SO₄ by Fe K-edge X-ray absorption near-edge structure (XANES). This adduct was prepared by first polarizing a Teflon bonded electrode, incorporating the high-area FeTMPP/BP material, at a potential at which the adsorbed macrocycle is present in the reduced state, followed by bubbling CO into the electrolyte. The resulting in situ XANES displayed two new preedge features centered at 7112 and 7115 eV, as found for other well-characterized iron macrocycle–CO adducts, as well as a shift of the main absorption edge toward higher values (ca. 1.3 V) indicative of charge transfer from the iron to CO. Dissociation of the adduct could be achieved by polarizing the electrode at more positive potentials to yield the CO-free form of the macrocycle in the ferric state, as has been reported for solution-phase CO–Fe porphyrin adducts in nonaqueous media.

Introduction

A number of transition-metal macrocycles, particularly those containing iron and cobalt centers, have been found to promote the rates of oxygen reduction in aqueous electrolytes when adsorbed or dispersed on carbon electrodes.¹ Despite years of research, little is known about the microenvironmental factors that control the electrocatalytic activity of this unique class of materials. Progress in this area has been hampered by the lack of structural and spectroscopic probes with sufficient sensitivity and specificity to detect and identify short-lived, adsorbed intermediates in situ. Particularly noteworthy are the efforts of Anson and co-workers,² who developed a theoretical formalism to extract information regarding macrocyclic–O₂ adducts based on cyclic voltammetric measurements.

Insight into electronic and steric factors of the electrocatalytic active site(s) could, in principle, be gained by examining the properties of macrocyclic adducts with other simple diatomics, such as CO and NO. This specific strategy has met with much success in studies involving synthetic models of hemoproteins responsible for the transport of dioxygen in living organisms.³

This paper describes the synthesis and characterization of a CO–Fe porphyrin adduct adsorbed on a high-area carbon electrode in an aqueous electrolyte. Evidence for the formation of this species was obtained from in situ Fe K-edge X-ray absorption near-edge structure (XANES) measurements, which showed, in addition to a shift in the main absorption edge toward higher energies compared to the CO-free ferrous porphyrin, two distinct features in the preedge region characteristic of genuine solid-state and solution-phase CO–Fe porphyrins adducts.⁴ Analysis of the in situ Fe K-edge XANES as a function of the applied potential revealed that the oxidation potential for this adsorbed adduct is shifted toward more positive values compared to the CO-free analogue, yielding the ferric form of the macrocycle, and presumably unbound CO, as the products. This behavior is very similar to that observed for closely related iron

porphyrins in nonaqueous solution phase by Saveant and co-workers⁵ and Kadish and co-workers,⁶ who generated the adduct by reducing electrochemically the macrocycle in CO-saturated solutions, thereby avoiding problems derived from the preparation and handling of highly oxygen-sensitive ferrous porphyrins.

Experimental Section

(5,10,15,20-Tetrakis(4-methoxyphenyl)-21*H*,23*H*,-porphine)-iron(III) chloride (FeTMPPCl, Aldrich Chemical) was adsorbed on Black Pearls (BP) high-area carbon, which had been heat-treated at 800 °C in a flowing Ar (UHP, Matheson) atmosphere for 2 h. For these experiments about 0.5 g of BP was added to a solution made by dissolving 0.15 g of FeTMPPCl in 0.5 L of acetone. After 20 h of continuous stirring, the mixture was rapidly filtered by suction (Whatman, qualitative no. 2). The amount of adsorbed material was determined by evaporating to dryness the filtered solution and subtracting the weight from that of the original amount of FeTMPPCl used, yielding about 19% w/w FeTMPPCl/BP. About 2 mg of this material was thoroughly mixed with an emulsified Teflon suspension (0.5 mg of Teflon, T30B, Dupont) and subsequently pressed onto the lower section of a piece of a hydrophobic carbon layer (4 × 8 mm² Eltech Systems), which served as the current collector. A reversible hydrogen electrode in the same solution (RHE), separated from the main cell compartment by a sintered glass frit, was used as a reference electrode. Experiments were conducted in aqueous 0.05 M H₂SO₄ prepared by diluting the as-received concentrated acid (5 N, Aldrich) in Nanopure 18-MΩ water. For the CO-binding measurements, the acid solution was purged with gaseous CO (5 N, Matheson) for about 2 h.

XANES were acquired at beamline 4-1 at the Stanford Synchrotron Radiation Laboratory (SSRL) operating at an energy of 3 GeV with a ring current of 60–100 mA. The beam was monochromatized with a set of two Si(111) crystals with the exit slit adjusted to 1 × 6 mm². All the measurements were performed in the fluorescence mode using a Lytle-type ioniza-

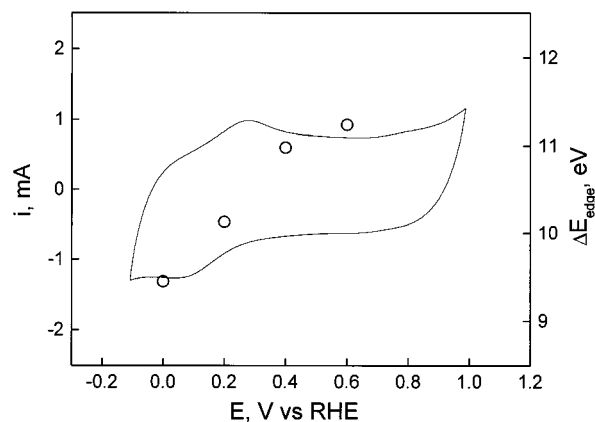


Figure 1. Cyclic voltammogram of a Teflon bonded 19% w/w FeTMPP/BP electrode in 0.05 M H₂SO₄ obtained in the same cell in which the in situ XANES experiments were performed at a scan rate of 2 mV/s. The open circles in this figure represent the shift in the main absorption edge referenced to metallic Fe ($\Delta E_{\text{edge}} = E_{\text{edge}} - E_{\text{Fe}}$; see text for detail, right ordinate) as a function of the applied potential.

tion detector purged with Ar with a 3-absorption-length (μ_x) Cr filter. The energy was calibrated using an iron foil of 1 μ_x , for which the first inflection point E_{Fe} is at 7112 eV. The position of the absorption edge (E_{edge}) is defined in this work as the energy at which the normalized absorption (fluorescence) is precisely one-half.

Results and Discussion

Figure 1 shows a cyclic voltammogram of a 19% w/w FeTMPPCl/BP electrode in 0.05 M H₂SO₄ at a scan rate of 2 mV/s recorded in the same cell in which the in situ XANES were acquired. As indicated, the adsorbed macrocycle displays a slightly irreversible redox peak with E_{ave}° of ca. 0.17 V versus RHE, in agreement with the results obtained for adsorbed (FeTMPP)₂O on BP in the same electrolyte.⁷ On the basis of extended X-ray absorption fine structure (EXAFS) studies⁷ performed in this laboratory, (FeTMPP)₂O, in this very acidic electrolyte, is present in both the reduced and oxidized states as a monomeric species coordinated axially either by water or by anions. It seems, thus, reasonable to assume that the same two species are responsible for the cyclic voltammetric features in Figure 1.

Also in agreement with data reported previously^{7,8} are the changes in the in situ XANES induced by the reduction of the adsorbed macrocycle. In particular, Figure 2 shows a series of in situ XANES obtained at 0.60, 0.40, 0.20, and 0.00 V, that is, within the potential range in which the redox changes occur. As clearly evidenced by these results, the reduction of the adsorbed macrocycle gives rise to a rather prominent peak at ca. 7117 eV accompanied by the disappearance of the preedge peak centered at ca. 7114 eV. In addition, it brings about a shift in E_{edge} toward lower energies of ca. 2 eV, as illustrated in Figure 1, which gives a plot of ΔE_{edge} versus potential (see open circles and right ordinate), where $\Delta E_{\text{edge}} = E_{\text{edge}} - E_{\text{Fe}}$.

After such measurements were completed, the adsorbed macrocycle was fully reduced by polarizing the electrode at 0.0 V, and CO was then bubbled into the electrolyte. Marked changes in the in situ XANES were found during this procedure, as evidenced by the results shown in Figure 3 collected before (a: dotted line) and after 20 min (b: dashed), and 2 h (c: solid) of CO purging. These include the appearance of two clearly defined preedge peaks centered at 7112 and 7115 eV, clearly seen in an expanded scale in panel B in this figure, a sizable

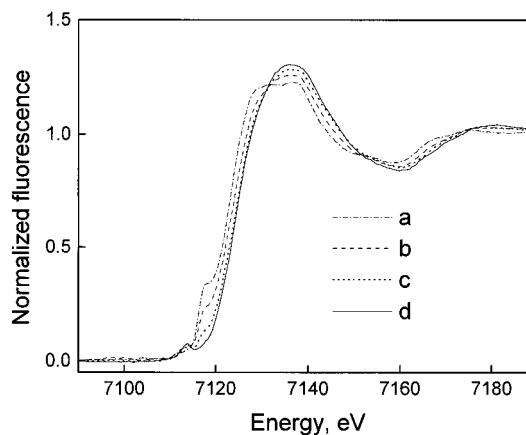


Figure 2. Series of in situ Fe K-edge XANES obtained for 19% w/w FeTMPP/BP at different potentials in 0.05 M H₂SO₄: 0.0 (a, dot-dash), 0.20 (b, dashed line), 0.40 (c, dotted line), and 0.60 V vs RHE (d, solid line).

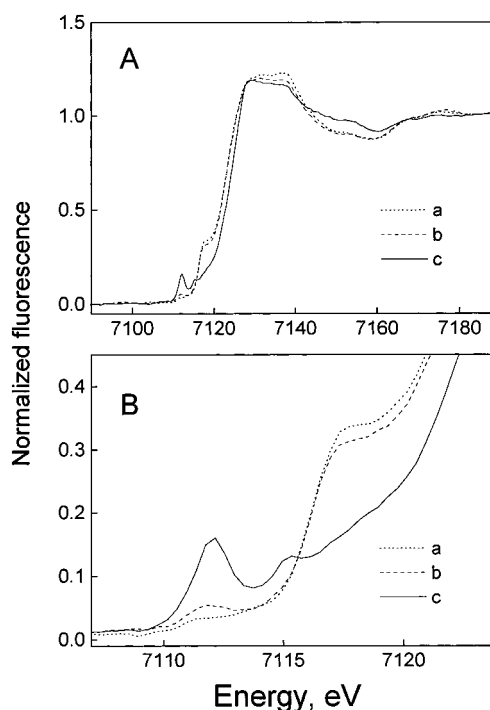
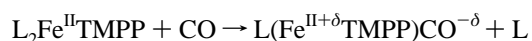


Figure 3. In situ Fe K-edge XANES of 19% w/w FeTMPPCl/BP polarized at 0.0 V vs RHE in 0.05 M H₂SO₄ before (a, dotted line) and after bubbling CO into the electrolyte for 20 min (b, dashed line) and 2 h (c, solid line) in the region 7090–7190 eV (A). Panel B shows the same plots in expanded form for clarity.

decrease in the prominent shoulder at 7117 eV, characteristic of the reduced form of the macrocycle, and a shift in E_{edge} toward higher energies. All these observations are consistent with the formation of a L(FeTMPP)CO adduct, where L is most probably water bound to Fe at the other axial position, that is,



In particular, the following items are noted.

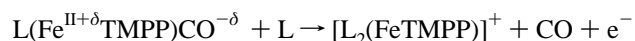
(i) Two preedge peaks separated by ca. 2.2 eV have been reported in the ex situ Fe K-edge XANES of a series of carbonyl basket-handle Fe(II) porphyrin adducts structurally characterized by X-ray diffraction, both in the solid state and in toluene solutions.⁴ Peaks in this preedge energy region are ascribed to partially allowed dipole-forbidden $1s \rightarrow 3d$ transitions. Depending on the nature of the ligand and spin state of the iron,

the spectra can display a single broad feature, as in the case of square-pyramidal halogeno or μ -oxo-Fe(III) porphyrins, or a well-defined doublet, as found for the monomeric Fe porphyrin CO adduct referred to above. According to Cartier et al.,^{4b} the presence of this doublet is most likely due to the low spin character of the iron center in the CO adduct. On the basis of quantum-mechanical calculations and polarized XANES measurements in the solid state, the preedge peaks at the lower and higher energies, denoted as P_1 and P_2 , respectively, are attributed to transitions to empty orbitals with pronounced d_{z^2} (P_1) character and with significant mixing of the π^* orbital of CO with the $d_{xz,yz}$ orbitals of the metal (P_2).

(ii) A shift in the absorption edge toward higher energies and the presence of much less resolved preedge features have been reported in the (static) spectra of deoxymyoglobin (Mb) and MbCO at pH 7.6 in 0.1 M phosphate buffer and an excess of sodium dithionite, following formation of the MbCO adduct.⁹ This observation is consistent with charge transfer from the ferrous center to the axially bound CO to render the iron site in a more oxidized state. Very similar effects have been reported in the case of Ni 2,3,9,10-tetramethyl-1,4,8,11-tetraazatetradecane (HTIM) by Furenli et al.,¹⁰ for which addition of CO to electrochemically prepared Ni(I)HTIM⁺ resulted in a shift in E_{edge} toward higher energies attributed by these authors to charge transfer from the metal to the ligand.

(iii) The rather large intensity of the preedge peak(s) appears consistent with a less symmetric environment surrounding the Fe site and, thus, with the formation of a mono as opposed to a bis CO adduct, as suggested above, although the coexistence of both species cannot be ruled out. Correlations between the energy and splitting, and intensity distributions of the $1s \rightarrow 3d$ preedge feature, and among the spin state, oxidation state, geometry, and bridging ligation of the iron site for a large number of inorganic iron complexes have been recently reported by Westre et al.¹¹

A series of in situ XANES were then acquired with the electrode polarized in sequence at 0.2, 0.4, and 0.6 V versus RHE (see Figure 4). In direct contrast to the results obtained for the adsorbed macrocycle in the absence of CO, very small differences could be discerned in this case between the in situ XANES at 0.0 and 0.2 V. At more positive potentials (e.g., 0.4 V), however, the two preedge features decreased, disappearing completely at 0.6 V versus RHE, and a new peak emerged centered at about 7113 eV. These spectral modifications appear consistent with the reaction



Some indication that a fraction of the macrocycle may still be present in the $L(\text{FeTMPP})\text{CO}$ form at this potential is provided by the presence of a slight, albeit unambiguous, shoulder at 7128 eV and by the broader character of the peak at 7113 eV compared with that found for the CO-free macrocycle in the oxidized state (see solid line in Figure 2).

It becomes evident from these results that the presence of axially bound CO modifies the redox properties of the reduced macrocycle. Similar observations have been reported by Saveant and co-workers⁵ and Kadish and co-workers⁶ for the closely related iron tetrakis(phenylporphyrin) (FeTPP) and brominated derivatives^{6b} in nonaqueous solution-phase electrolytes. As shown by these workers, addition of CO causes a shift in the voltammetric peak ascribed formally to the Fe(II)-TPP/Fe(III)TPP couple by more than 0.3 V toward more positive values. In fact, no clearly defined redox features could be discerned in the cyclic voltammogram of adsorbed $L(\text{FeTMPP})$ -

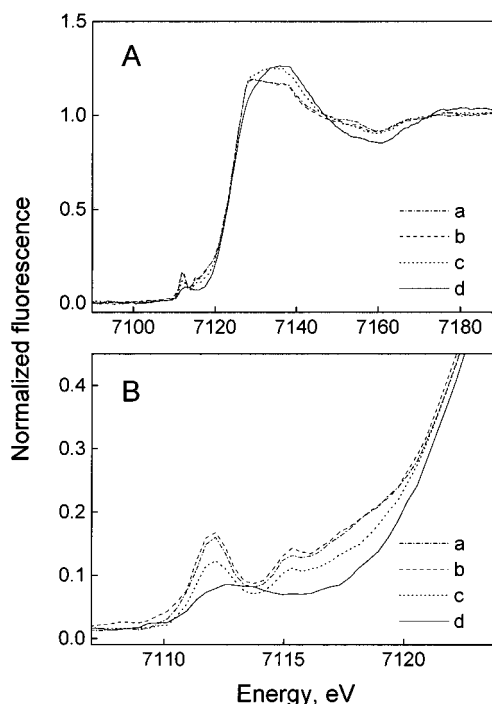


Figure 4. Series of in situ XANES acquired with a 19% w/w FeTMPP/BP with the electrode polarized in sequence at 0.0 (a, dot-dash line), 0.2 (b, dashed line), 0.4 (c, dotted line), and 0.6 V vs RHE (d, solid line) after bubbling CO into a 0.05 M H_2SO_4 solution for over 2 h with the electrode polarized at 0.0 V vs RHE (A). Panel B shows the same plots in expanded form for clarity.

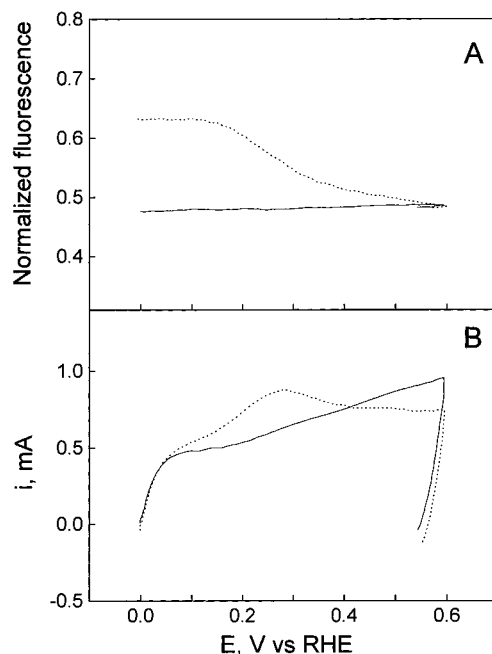


Figure 5. Real-time normalized fluorescence intensity at a fixed energy of 7122.5 eV recorded while the potential was scanned at 2 mV/s between 0.0 and 0.6 V vs RHE (A) for 19% w/w $L(\text{FeTMPP})\text{CO}/\text{BP}$ (solid line) and 19% w/w FeTMPP/BP (dotted line) after holding the potential at 0.0 V vs RHE for 30 min. Other conditions are given in the caption of Figure 1. The corresponding linear-scan voltammograms acquired simultaneously are shown in panel B in this figure.

CO, prepared by polarizing the electrode at 0.0 V and bubbling CO for 30 min in the same electrolyte, in the region in which the CO-free analogue shows an oxidation peak (compare solid versus dotted line in solid curve in Figure 5B). Instead, an almost linear increase in the current was observed between 0.2

and 0.6 V attributed in all likelihood to the kinetically hindered oxidation of L(FeTMPP)CO. During this linear potential scan, the fluorescence intensity was monitored at a fixed energy of 7122.5 eV, that is, very close to the absorption edge of the adsorbed CO-free FeTMPP, to determine more precisely and in real time possible shifts in E_{edge} induced by the oxidation of L(FeTMPP)CO. As shown by the solid lines in Figure 5A, no changes in the normalized fluorescence intensity, and, hence, in E_{edge} , could be discerned over the entire potential range examined. This observation supports the view that the iron center in L(FeTMPP)CO is in an oxidized state. In fact, the near coincidence of the value of NF at 0.6 V for L₂(FeTMPP) and L(FeTMPP)CO is consistent with the fact that a single species is present at that potential.

It may be expected that the binding of CO to FeTMPP will block the active site for dioxygen reduction and, therefore, render the electrocatalyst inactive for this process. Strongly inhibitory effects have been reported by Gupta et al.¹² for iron tetrasulfonated phthalocyanine (FeTsPc), a potent four-electron electrocatalyst for O₂ reduction, adsorbed on ordinary pyrolytic graphite electrodes in aqueous 0.1 M NaOH upon addition of CN⁻, which is isoelectronic with CO. As shown by those workers, the onset potential for O₂ was found in that case to be as negative as that found for bare OPG in the same electrolyte. In fact, only very small currents could be detected upon polarizing the L(FeTMPP)CO/BP electrode at 0.0 V while bubbling O₂ into the electrolyte. However, a more detail investigation of such effects seemed beyond the scope of the present study and was not pursued further.

An extension of this work to include in situ Fe K-edge extended X-ray absorption fine structure (EXAFS) could be used to determine bond distances between the Fe center and carbon in CO. It may thus be envisioned that information derived from in situ XAFS for these (and other simple) adducts will help elucidate long-sought structure–activity relations for these materials as dioxygen electrocatalysts in aqueous solutions.

Acknowledgment. This work was supported by the Advanced Research Projects Agency, ONR Contract No. N00014-92-J-1848.

References and Notes

- (1) See, for example, the following. (a) Zagal, J.; Sen, R. K.; Yeager, E. B. *J. Electroanal. Chem.* **1977**, *83*, 207–213. (b) Zagal, J.; Bindra, P.; Yeager, E. B. *J. Electrochem. Soc.* **1980**, *127*, 1506–1517. (c) Collman, J. P.; Denisevich, P.; Konai, Y.; Marrocco, M.; Koval, C.; Anson, F. C. *J. Am. Chem. Soc.* **1980**, *102*, 6027–6036. (d) Shigehara, K.; Anson, F. C. *J. Phys. Chem.* **1982**, *86*, 2776–2783. (e) Durand, R. R., Jr.; Bencosme, C. S.; Collman, J. P.; Anson, F. C. *J. Am. Chem. Soc.* **1983**, *105*, 2710–2718. (f) Tanaka, A. A.; Fierro, C.; Yeager, E. B.; Scherson, D. *J. Phys. Chem.* **1987**, *91*, 3799. (g) Tanaka, A. A.; Fierro, C.; Scherson, D. A.; Yeager, E. B. *Mater. Chem. Phys.* **1989**, *22*, 431–456.
- (2) Xie, Y.; Kang, C.; Anson, F. C. *J. Chem. Soc., Faraday Trans.* **1996**, *92*, 3917.
- (3) See, for example, the following. Momenteau, M. *Pure Appl. Chem.* **1986**, *58*, 1493.
- (4) (a) Ascone, I.; Bianconi, A.; Dartyge, E.; Della Longa, S.; Fontaine, A.; Momenteau, M. *Biochim. Biophys. Acta* **1987**, *915*, 168. (b) Cartier, C.; Momenteau, M.; Dartyge, E.; Fontaine, A.; Tourillon, G.; Bianconi, A.; Verdager, M. *Biochim. Biophys. Acta* **1992**, 169.
- (5) (a) Croisy, A.; Lexa, D.; Momenteau, M.; Saveant, J. M. *Organometallics* **1985**, *9*, 1574. (b) Balducci, G.; Chottard, G.; Gueutin, C.; Lexa, D.; Saveant, J.-M. *Inorg. Chem.* **1994**, *33*, 1972.
- (6) (a) Swistak, C.; Kadish, K. M. *Inorg. Chem.* **1987**, *26*, 405. (b) Tagliatesta, P.; Li, J.; Autret, M.; Van Caemelbecke, E.; Villard, A.; D'Souza, F.; Kadish, K. M. *Inorg. Chem.* **1996**, *35*, 5570.
- (7) Kim, S.; Tryk, D. A.; Bae, I. T.; Sandifer, M.; Carr, R.; Antonio, M. R.; Scherson, D. A. *J. Phys. Chem.* **1995**, *99*, 10359.
- (8) Kim, S.; Bae, I. T.; Sandifer, M.; Ross, P. N.; Woicik, J.; Antonio, M. R.; Scherson, D. A. *J. Am. Chem. Soc.* **1991**, *113*, 9063.
- (9) Mills, D. M.; Lewis, A.; Harootunian, A.; Huang, J.; Smith, B. *Science* **1984**, *223*, 811.
- (10) Furenliid, L. R.; Renner, M. W.; Fujita, E. *Physica B* **1995**, 208–209, 739.
- (11) Westre, T. E.; Kennepohl, P.; DeWitt, J. G.; Hedman, B.; Hodgson, K. O.; Solomon, E. I. *J. Am. Chem. Soc.* **1997**, *119*, 6297.
- (12) Gupta, S.; Fierro, C.; Yeager, E. B. *J. Electroanal. Chem.* **1991**, *306*, 239.